ELSEVIER

Contents lists available at ScienceDirect

Structures

journal homepage: www.elsevier.com/locate/structures





Seismic-induced vibration control of modular high-rise buildings using mega modularized substructure

Linwei Jiang ^a, Haoran Zuo ^a, Kaiming Bi ^{b,c,*}, Hong Hao ^{a,d,**}, Wensu Chen ^a

- a Centre for Infrastructural Monitorine and Protection. School of Civil and Mechanical Engineering. Curtin University. Kent Street. Bentley. WA 6102. Australia
- ^b Department of Civil and Environmental Engineering, The Hong Kong Polytechnic University, Kowloon, Hong Kong, China
- c Research Centre for Urban Hazards Mitigation (RCUHM), The Hong Kong Polytechnic University, Kowloon, Hong Kong, China
- d Guangdong Provincial Key Laboratory of Earthquake Engineering and Applied Technology, Earthquake Engineering Research and Test Center, Guangzhou University, Guangzhou, China

ARTICLE INFO

Keywords: High-rise buildings Modularization technique Mega modularized substructure Vibration control

ABSTRACT

Modular construction technique is becoming more and more popular in engineering community since it offers significant advantages like reduced environmental impact, enhanced quality control, and faster construction speed compared to traditional onsite construction methods. However, its application in high-rise buildings remains limited due to significant concerns like the reliability of the structural system. To address this challenge, this study proposes a novel solution, i.e., a mega modularized substructure, for modular high-rise buildings. This system originates from the conventional mega substructure configuration and integrates prefabricated modular units connected by inter-module connections into the mega frames. The structural properties of the inter-module connections are optimized based on the tuned mass damper (TMD) concept, with the mean squared displacement response of the primary structure as the control objective in the optimization analysis. With the optimized parameters, the mega modularized substructure demonstrates favorable attenuation of primary structural responses in multiple modes and enhances the control effectiveness of structures compared to the conventional mega substructure. Furthermore, the present study investigates the robustness of the proposed system against the malfunction of the modular substructure and pounding between modules and between modules and frame on control effectiveness, thereby validating its suitability for application in construction of high-rise frame structures.

1. Introduction

In the past decades, significant advancements in the fields of material and construction techniques have revolutionized the design and construction of high-rise structures [1]. High-rise buildings are not only architecturally appealing but also provide a practical solution to the land scarcity challenges in densely populated countries/regions. Consequently, there has been a notable global trend towards the construction of high-rise even super-high-rise buildings [2], and many high-rise structures have become iconic landmarks of a city, such as the Burj Khalifa in Dubai and the Empire State Building in New York.

High-rise buildings, which are inherently slender and flexible, are particularly susceptible to vibrations induced by seismic excitations

compared to low-/middle-rise buildings. Consequently, substantial research has been conducted to employ various types of control techniques to alleviate the vibrations. These techniques can be generally classified into three categories: passive, active, and semi-active [3]. Their respective control algorithms and pros and cons are summarized as follows: (1) Passive control devices operate independently of external energy input, rendering them to continue controlling vibrations during severe seismic events when power systems fail. Various types of passive control techniques have been developed, including TMDs [4], tuned liquid column dampers [5], visco-elastic dampers [6], and base isolation techniques [7]. Due to their straightforward implementation and effective control, passive control techniques find widespread applications in high-rise buildings. However, passive control techniques are

E-mail addresses: Kaiming.bi@polyu.edu.hk (K. Bi), haohong@gzhu.edu.cn (H. Hao).

^{*} Corresponding author at: Department of Civil and Environmental Engineering, The Hong Kong Polytechnic University, Kowloon, Hong Kong, China.

^{**} Corresponding author at: Guangdong Provincial Key Laboratory of Earthquake Engineering and Applied Technology, Earthquake Engineering Research and Test Center, Guangzhou University, Guangzhou, China.

only effective within specific frequency ranges, and their performance in mitigating seismic-induced vibrations may not always be optimal under wide-band seismic ground motions. (2) In contrast to passive control techniques, active control technique requires an external energy source to mitigate vibrations in civil structures. Generally, the active control devices comprise a series of actuators and sensors, with control forces determined based on the structural response. Various types of active control devices have been proposed and utilized in practice, such as active mass dampers [8], active bracing systems [9], and active connected building systems [10]. The adaptability of control forces in response to structural responses allows active control devices to remain effective across a broad frequency range for seismic excitations. However, concerns like installation complexity, potential instability, and high costs are significant considerations for this control strategy. (3) To diminish the reliance on external energy in active control technique, semi-active control was introduced by Hrovat et al. [11]. This control strategy aims to reduce structural responses by combining the benefits of both passive and active control strategies. Semi-active control technique offers the adaptability of their active counterpart while minimizing energy consumption, making them capable of operating on battery power-a crucial feature considering potential power system failures during extreme events. Various types of semi-active control devices, such as variable-orifice dampers [12], controllable-fluid dampers [13], and semi-active impact dampers [14] have been developed. Previous studies have confirmed that semi-active devices can outperform passive counterparts under dynamic loading scenarios [15,16]. In general, both semi-active and active control strategies have the potential for superior control performance compared to passive types. However, their inherent complexity, potential instability, and reliance on energy input are notable disadvantages. In contrast, passive control devices, which are simple and effective in mitigating structural vibrations, do not require external power input, therefore, they are widely applied in practice.

As an effective passive control strategy, the mega substructure configuration, a concept initially introduced by Feng et al. [17], is a reliable option to mitigate the vibrations of high-rise buildings. This system mainly comprises two components: the primary structure and the secondary substructure. By tuning the dynamic characteristics of the secondary substructure, seismic energy can be transferred from the primary structure to the substructure and dissipated with conventional damping devices. Consequently, the secondary substructure functions as a TMD with a significantly larger mass ratio compared to the conventional small-scale TMD, which could enhance the effectiveness of this control system. Furthermore, the mega substructure system exhibits remarkable control robustness against variations in structural properties and external dynamic excitations. Given these notable features, this system is widely applied in high-rise buildings, and various types of mega substructure systems have been developed in the past decades, such as the mega frame with suspended floors [18] and core-tube with suspended floors [19].

Modular construction involves prefabricating structural components offsite in a factory, followed by the assembly work at the construction site. This technique offers notable benefits such as accelerated manufacturing, enhanced quality control, and reduced environmental impact compared to the traditional onsite construction methods [20, 21]. The benefits of modular construction are particularly pronounced in high-rise buildings due to the increased number of modular units. While the modular construction technique has been widely adopted in low- and middle-rise buildings [22], its application to high-rise buildings remains limited (the proportion is less than 1 %) [23]. A key obstacle hindering its widespread adoption is the absence of reliable structural systems [23].

Currently, three structural systems are predominantly adopted for modular high-rise buildings: the core, podium, and infilled frame systems [24]. In core-based modular high-rise buildings, prefabricated modular units are grouped around stable cores designed to resist vertical loads, and lateral loads are also transferred to the cores [25]. In the

podium system, modules are placed on the podium, which serves as a foundation to support the prefinished modules. This system is preferable for mixed-use buildings, offering convenience for retail or commercial purposes [26]. In the infilled frame system, modular units are positioned between the beams and columns of the frame structure, which can be constructed using conventional onsite construction methods to ensure the overall stability of the modular building. Despite the availability of these structural systems for modular high-rise buildings, the challenge of a lack of reliable structural systems still waits to be addressed.

To advance the modular construction technique in high-rise buildings, the present study introduces a novel structural system designed specifically for modular high-rise buildings, termed "mega modularized substructure" hereinafter. This system is derived from the conventional mega substructure configuration, where flexible modular substructures are placed between the beams and columns of the primary structure. In this system, the primary structure can be constructed using conventional onsite construction methods, ensuring the overall stability of the mega modularized substructure. Once the construction of the primary structure is completed, prefabricated modules can be transported from the factory to the construction site for assembly. Since the modules can be considered as individual masses, therefore, their connections can be tuned to make them behave as multiple tuned mass dampers to control the vibrations of the primary structure. All the connections between the modules and the primary structure, as well as the inter-module connections, can be properly tuned to achieve the best control effectiveness.

Compared to the existing three modular high-rise building systems, the proposed mega modularized substructure possesses the following advantages: (1) Since the modules in the mega modularized substructure can behave like TMDs and the mass ratio between the secondary and primary structures can be up to a remarkable level (e.g., 1.0), the structural responses can be more effectively mitigated. (2) The modules on different floors can be regarded as vertically distributed TMDs, leading to multi-mode vibration control effect of this system [27], which further enhances the control effectiveness of the mega modularized substructure. (3) Since the multiple modules are connected together, the malfunction of a single connection (even a few connections) will not obviously diminish the control effectiveness, i.e., the control system is robust against the malfunction of the secondary structure. Due to these advantages, the mega modularized substructure could address the global stability and structural robustness concerns of conventional modular high-rise buildings to offer a feasible, reliable, and robust option for modular high-rise buildings.

This paper investigates the effectiveness of the proposed mega modularized substructure on vibration control of the structure during earthquake ground shaking. The paper is organized as follows: the detailed configuration of the mega modularized substructure is presented in Section 2; the analytical model and parameter optimization are discussed in Section 3; the details of numerical models are presented in Section 4; the control effectiveness and further exploration into robustness and the influences of pounding between modules and between modules and the frame structure are discussed in Section 5; and the conclusions are summarized in Section 6.

2. Concept of the mega modularized substructure

Fig. 1(a) illustrates a conventional mega substructure system, which is the prototype structure in Ref. [17]. As depicted, this system consists of two components: the mega frame and the substructure. During excitations such as wind or earthquakes, the primary structure, i.e., the mega frame, transfers kinetic energy to the substructure, and the energy is dissipated by the conventional damper systems. This concept is similar to the widely used TMD in the field of structural vibration control. However, due to the large mass ratio between the substructure and the primary structure, this is a large-scale TMD system, and it is more robust in terms of control effectiveness than the traditional small-scale TMD. This property is highly appealing and renders the system practical in

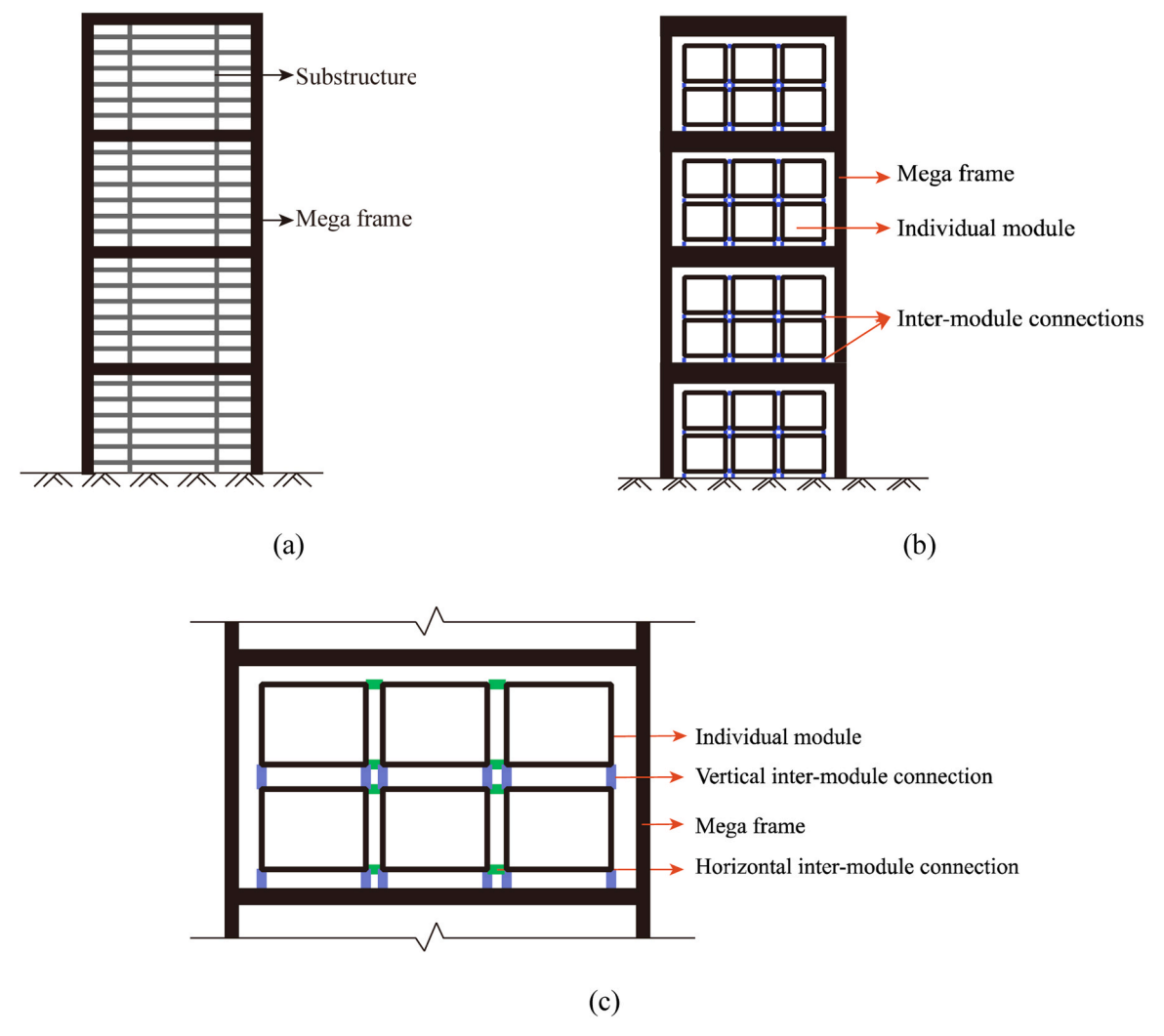


Fig. 1. Schematics of (a) conventional mega substructure, (b) mega modularized substructure, and (c) inter-module connection details.

engineering applications, especially given the significance of vibration control in high-rise buildings.

Inspired by the mega substructure system, the present study proposes an innovative mega modularized substructure designed for mitigating vibrations in modular high-rise buildings as depicted in Fig. 1(b). To develop the mega modularized substructure, the substructure in the conventional mega substructure system is replaced by prefabricated modular units. During on-site construction, the mega frame can be constructed first, followed by stacking modules between the floors of the mega frame. The modular substructure consists of multiple layers of modules stacked on top of each other, with each layer incorporating several modules that are connected by the inter-module connections (as shown in Fig. 1(c)). In that case, the number of modules on each floor is limited so that the stability of the substructure can be straightforwardly maintained, which allows the adaptation of modular constructions in high-rise buildings.

Furthermore, the modules can be used as multiple TMDs for vibration control by connecting them to the primary structure with a type of energy-dissipating inter-module joint. While conventional inter-module connections [28,29] only account for the stiffness contribution of the joints to the structural behavior, the effect of both the stiffness and damping properties of the joint on the structural response is considered in the present study. Consequently, the modules in the proposed mega modularized substructure serve as dynamic vibration absorbers to dissipate seismic energy. Thereby, the proposed system can facilitate the construction of modular high-rise buildings and mitigate the vibrations

of the structure.

In summary, the proposed mega modularized substructure has the following characteristics:

- (1) The energy-consuming inter-module connections enable the modules themselves to function as TMDs, effectively mitigating the response of both the primary and secondary structures under seismic excitations.
- (2) The mass ratio in this system has the potential to be significantly larger than that in a conventional TMD system. A higher mass ratio indicates the possibility of achieving better control effectiveness and robustness of the system.
- (3) The modular substructure inherently possesses multiple vibration modes, signifying the absorption of energy over a broad frequency band. This characteristic enhances the effectiveness of the control system under seismic ground motions, as seismic energy typically distributes in a wide band of frequencies.

3. Analytical model and parameter optimization

3.1. Analytical model

In the present study, to showcase the control effectiveness of the mega modularized substructure, the dynamic responses are examined and compared with those of the mega substructure system. For the sake of simplicity, yet maintaining generality, two layers of modular units in

a floor are assumed, with each layer having three modules, resulting in a total of six modules in a floor. It should be noted that in practice there should be a greater number of modules than six on each floor. However, to simplify the analysis, only six modules are assumed in the present study. This can be achieved in practice to rigidly connect some individual modules to form six super modules.

Fig. 2 shows the analytical model of the mega modularized substructure. In this model, the mega structure and the substructure are represented as a single-degree-of-freedom (SDOF) system and a multiple-degree-of-freedom (MDOF) system, respectively. The parameters in Fig. 2 are explained as follows: M refers to the fundamental modal mass of the mega frame; m represents the mass of a single module; Kdenotes the fundamental modal stiffness of the mega frame; C is the corresponding modal damping; k_s and c_s are the shear stiffness and damping coefficient of the vertical inter-module connection, respectively; k_a and c_a are the axial stiffness and damping coefficient of the horizontal inter-module connection, respectively. Notably, the vertical and horizontal inter-module connections are assumed to have identical properties in the present study. This assumption was made mainly from the practical point of view. It is obvious that the manufacture and installation efforts would be significantly increased if one connection is different from the other, making it not practical in engineering practices. Moreover, this simplification would also facilitate the convergence of parameter optimization: if the parameters of the connections are different from each other, a lot of parameters need to be optimized, which would significantly increase the optimization effort. Therefore, to facilitate the following derivation, k_s and k_a are represented by k_s and c_s and c_a are denoted by c_a , respectively.

The equation of motion of this system thus can be written as

$$M\ddot{x} + C\dot{x} + Kx = F\# \tag{1}$$

where M, C, and K are the mass, damping, and stiffness matrices, respectively, F is the force vector, and x is the displacement vector relative to the ground. The overdots denote the derivative of displacement with respect to time.

For the system shown in Fig. 2, the mass matrix is $\mathbf{M} = \text{diag}[M, m, m, m, m, m, m]$, and the stiffness matrix \mathbf{K} can be expressed as

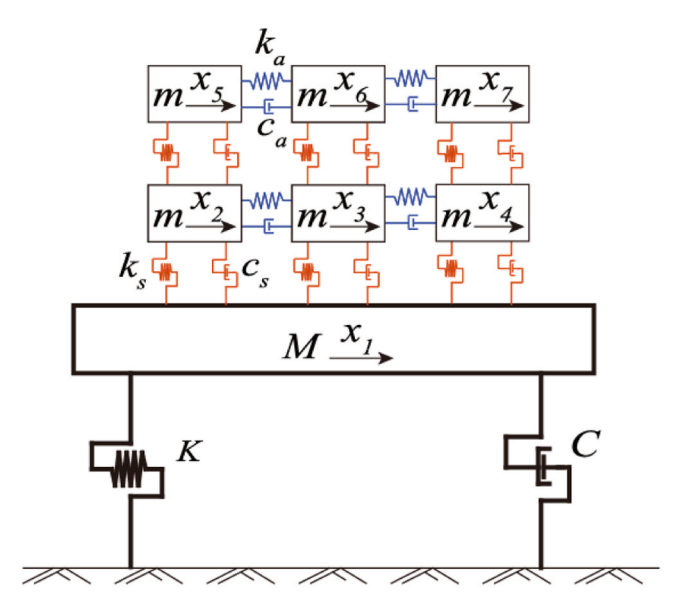


Fig. 2. Analytical model of the mega modularized substructure.

$$\mathbf{K} = \begin{bmatrix}
K + 3k & -k & -k & -k & 0 & 0 & 0 \\
-k & 3k & -k & 0 & -k & 0 & 0 \\
-k & -k & 4k & -k & 0 & -k & 0 \\
-k & 0 & -k & 3k & 0 & 0 & -k \\
0 & -k & 0 & 0 & 2k & -k & 0 \\
0 & 0 & -k & 0 & -k & 3k & -k \\
0 & 0 & 0 & -k & 0 & -k & 2k
\end{bmatrix} #$$
(2)

The damping matrix C has the identical structure as K with the elements K and k replaced by C and c, respectively.

When the structure is subjected to an earthquake ground motion, the equation of motion can be modified as

$$M\ddot{\mathbf{x}} + C\dot{\mathbf{x}} + K\mathbf{x} = -\mathbf{M}\mathbf{r}\mathbf{a}^{\#} \tag{3}$$

where r is the influence vector and it is [1, 1, ..., 1] for the external ground motion, and a is the ground acceleration.

Transferring Eq.(3) into the frequency domain, the displacement response can be derived as [30]:

$$\mathbf{H}_{\mathbf{Disp}}(\omega) = \left(-\omega^2 \mathbf{M} + \mathrm{i}\omega \mathbf{C} + \mathbf{K}\right)^{-1} \omega^2 \mathbf{M} \mathbf{r} H_{ug}(\omega) \# \tag{4}$$

where $H_{Disp}(\omega)$ is the displacement response in the frequency domain, $H_{ug}(\omega)$ is the power spectral density (PSD) of the ground displacement, and ω is the excitation frequency in rad/s. Similarly, the velocity and acceleration responses can be derived with linear combinations of $H_{Disp}(\omega)$ and $rH_{ug}(\omega)$, which are not presented herein for conciseness.

In the optimization analysis, the ground motion is normally considered as a white noise process with an intensity of S_0 . Therefore, the displacement transfer function and the mean squared displacement can be calculated by

$$\boldsymbol{H}(\omega) = \frac{\boldsymbol{H}_{\text{Disp}}(\omega)}{-\omega^2 \boldsymbol{H}_{\text{lg}}(\omega)} = -\left(-\omega^2 \mathbf{M} + i\omega \mathbf{C} + \mathbf{K}\right)^{-1} \mathbf{Mr} \boldsymbol{\#}$$
(7)

$$\delta_i^2 = \int_{-\infty}^{\infty} h_i(\omega) h_i^*(\omega) S_0 d\omega \quad (i = 1, 2, ..., 7) \#$$
 (6)

where $H(\omega)$ and ${\delta_i}^2$ are the displacement transfer function matrix and mean squared displacement of the ith degree of freedom, respectively, $h_i(\omega)$ refers to the transfer function of the ith displacement response corresponding to the ith column component of $H(\omega)$, and $h_i^*(\omega)$ is the conjugate of $h_i(\omega)$.

3.2. Parameter optimization set-up

The following parameters are defined to design the mega modularized substructure and evaluate its control effectiveness:

- (1) Mass ratio (R_m). The mass ratio is the ratio of the total mass of modules at a floor to the mass per floor of the mega frame, which is defined as $R_m = \frac{\sum_{i=1}^6 m_i}{M}$. Based on the conventional mega substructure design [17], a mass ratio of 1.0 is adopted in the present study.
- (2) Stiffness ratio (R_k). The stiffness ratio is the ratio between the inter-module connection stiffness and that of the mega structure defined as $R_k = k/K$. Once the optimal stiffness ratio is obtained, the stiffness of the inter-module connections can be easily decided.
- (3) Damping coefficient ratio (R_c). The damping coefficient ratio denotes the ratio between the inter-module connection damping coefficient and that of the mega structure defined as $R_c = c/C$. Similarly, when the optimal damping coefficient ratio is decided,

the damping coefficient of the inter-module connections can be obtained.

In the present study, the mean squared displacement of the mega structure $({\delta_1}^2)$ is selected as the optimization target to be minimized. It is obvious from Eq. (6) that ${\delta_1}^2$ can be calculated as follows:

$$\delta_1^2 = \int_{-\infty}^{\infty} h_1(\omega) h_1^*(\omega) S_0 d\omega \# \tag{7}$$

where $h_1(\omega)$ is the displacement transfer function of the mega structure and $h_1^*(\omega)$ is the corresponding conjugate counterpart of $h_1(\omega)$.

Substituting the mass, stiffness, and damping matrices of the mega modularized substructure in Section 3.1 into Eq. (7), it is observed that the mean squared displacement of the mega structure is only dependent on two variables, namely the stiffness ratio and damping coefficient ratio with the properties of the mega structure and the mass ratio predetermined.

The transfer function of the mega structure displacement response in Eq. (5) is extremely complex, making it challenging to obtain the closedform solutions of optimal stiffness and damping coefficient ratios. Therefore, in the present study, the numerical searching method, a commonly employed approach for damper optimization [27], is utilized to perform the optimization analysis in Matlab software. Numerical searching optimization was conducted with the gradient-based methods for long time [31]. The conventional gradient-based methods may introduce errors due to the discrete variables or indifferentiable objective functions, and the accuracy of the results relies on the initial guess [31]. Compared to gradient-based methods, genetic algorithms are powerful numerical searching techniques since they do not need a continuous and differentiable objective function [32]. Among the various genetic algorithms, non-dominated sorting genetic algorithm version II (NSGA-II) is an effective method for optimization problems both with and without constraints, and it can also balance computational cost and efficiency. Therefore, the NSGA-II genetic algorithm is adopted to conduct the optimization analysis, which is composed of three main operators namely selection, crossover, and mutation. The configuration parameters of the NSGA-II genetic algorithm used in this study are listed in Table 1.

4. Numerical models

To demonstrate the control effectiveness of the mega modularized substructure, the uncontrolled structure and the mega substructure as reported in Ref. [17] are selected as the reference structures for comparison as depicted in Fig. 3. The uncontrolled structure in Fig. 3(a) is a conventional four-story mega frame, which is 200 m in height. By incorporating the substructure between the floors of the mega frame, the mega substructure system can be formed as shown in Fig. 3(b) [17]. In the mega modularized substructure as proposed in the present study (as shown in Fig. 3(c)), the substructure in the mega substructure system is divided into six small modules connected by flexible inter-module connections. Table 2 tabulates the properties of the mega substructure system including the stiffness and damping coefficients of the substructure, which are optimally designed given a mass ratio of 1.0 in Ref. [17]. As discussed above, in practice there might be more than six small modules on each floor. Therefore, the modules in the mega

Table 1Configuration parameters of the NSGA-II genetic algorithm.

Parameters	Value
Maximum generation	100
Popoulation size	50
Crossover probability	0.8
Range of the optimization variables	$0 < R_k \le 1, 0 < R_c \le 1$

modularized substructure are referred to as super modules hereinafter to distinguish from the conventional small-scale modules in modular buildings.

Notably, the damping coefficient of the primary structure in Table 2 is calculated by assuming a constant damping ratio of 2 % for the first vibration mode. To determine the inter-module connection parameters of the modular substructure in the mega modularized substructure, the following three assumptions are made: (1) Only the first vibration mode of the primary structure is considered, and it is simplified as an SDOF system; (2) The total mass of the modular substructure is the same as that in the mega substructure system, i.e., R_m is 1.0 for the mega modularized substructure; (3) The stiffness and damping coefficients of the modular substructure on each floor are the same. Consequently, with the use of modal mass, stiffness, and damping coefficients of the primary structure, and the optimization methodology in Section 3, the stiffness and damping coefficients of the modular substructure can be calculated, which are tabulated in Table 3.

With the information provided in Tables 1 and 2, the finite element models of the uncontrolled structure, the mega substructure, and the mega modularized substructure can be established in OpenSees [33]. It should be noted that only the mass, stiffness, and height of the primary structure were reported in Ref. [17], and the geometry dimensions of the primary structure need to be calculated before the establishment of the finite element models. According to the inter-story stiffness and height given in Table 2, the moment of inertia I of each column of the primary structure is calculated by

$$I = \frac{Kh^3}{24E} \# \tag{8}$$

where h is the height of each floor and it is 50 m, E is the Young's modulus of materials and it is set as $3.45 \times 10^4 \text{ N/mm}^2$ in the present study. The column section is assumed to be square and the size a of the section can be obtained by

$$a = (12I)^{\frac{1}{4}}\# \tag{9}$$

Once the size of the column section is determined, the mass per length $m_{\rm column}$ is calculated by

$$m_{\text{column}} = \rho a^2 \# \tag{10}$$

where ρ is the material density and it is 2.5 t/m³. With the mass of the column being determined, the mass of the floor beam $m_{\rm floor}$ can be calculated by

$$m_{\text{floor}} = M - 2 \times 50 \times m_{\text{column}} = M - 100 m_{\text{column}} \#$$
(11)

Again, the section of the floor beam is assumed to be square, and the floor span length l is assumed as 20 m in the present study, therefore, the size b of the beam section is

$$b = \sqrt{\frac{m_{\text{floor}}}{\rho l}} \# \tag{12}$$

Similarly, the mass of the floor beam per length $m_{\rm column}$ is

$$m_{\rm column} = \rho b^2 \# \tag{13}$$

The detailed information of the primary structure is outlined in Table 4. With the data provided in the table, the numerical model for the primary structure can be established by employing the elastic beam-column element available in OpenSees. A convergence test is conducted, and the results indicate that an element length of 1 m can achieve a reasonable balance between computational efforts and accuracy. Consequently, this study adopts an element length of 1 m, leading to a total of 400 elements for the columns and 80 elements for the beams. For the sake of simplicity, the beam-column joint is assumed to be rigidly connected in this study. Also, the vertical column-to-column connection is simplified with the rigid link to simplify the analysis, which is a

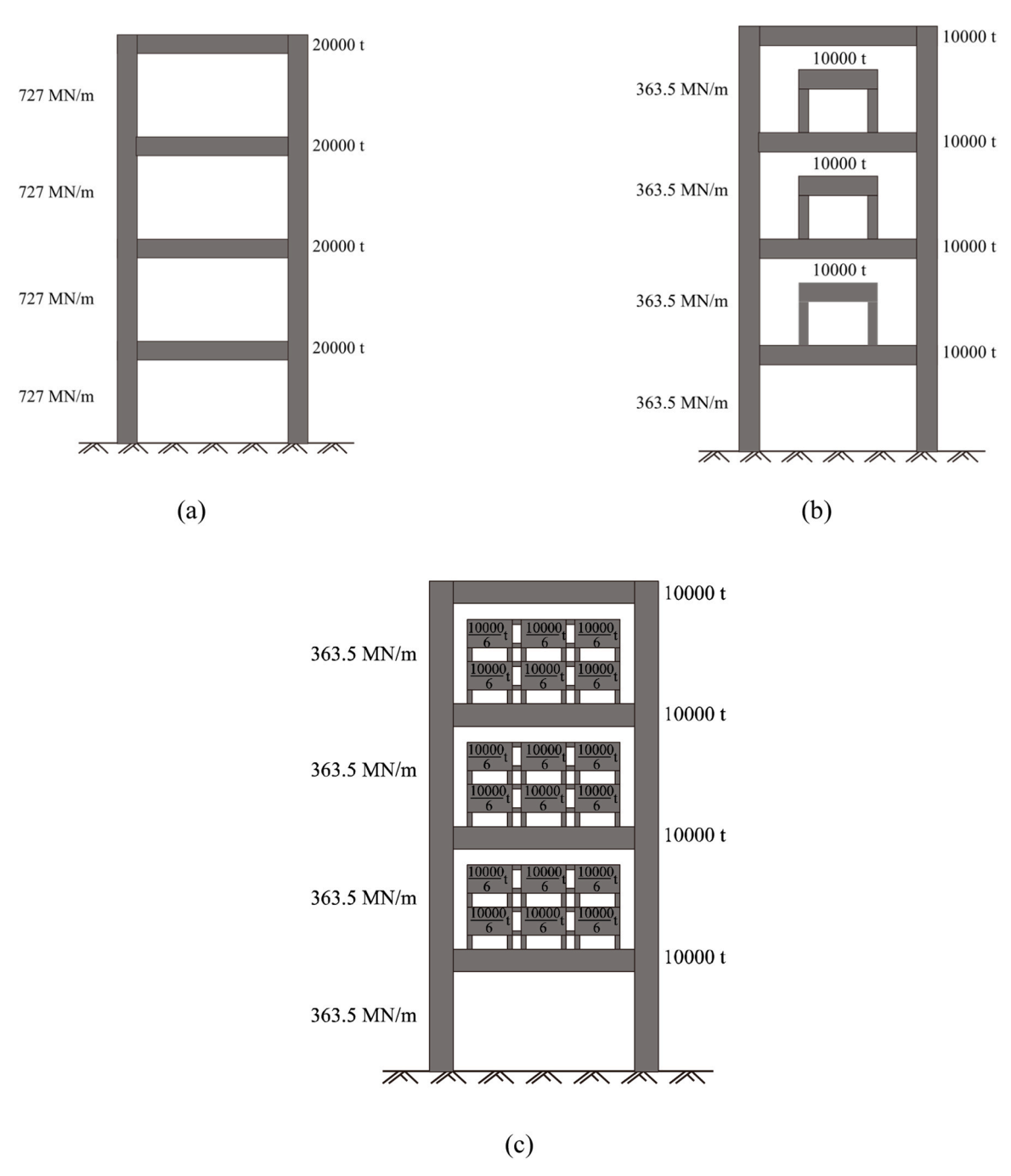


Fig. 3. Schematics of (a) prototype structure, (b) mega substructure system, and (c) mega modularized substructure.

common practice in many previous studies [34,35].

Regarding the substructure, both the modular units in the mega modularized substructure and the substructure in the conventional mega substructure are represented by the lumped mass and connected to the primary structure by the zero-length elements in OpenSees with parameters provided in Tables 1 and 2. Additionally, the inherent damping of the primary structure is formulated in the Rayleigh form with a damping ratio of 2 % for the first two vibration modes. Notably, only the horizontal response is considered in this study, while vertical and rotational responses are not considered. The schematics of the finite element models are illustrated in Fig. 4.

To validate the reasonability of the numerical models developed in this study, an eigenvalue analysis is performed to determine the natural frequencies of the developed finite element model of the primary structure. The fundamental period is calculated as 3.0 s, showing good

agreement with the analytical result in Ref. [17]. In addition, the fundamental mode shape of the primary structure is shown in Fig. 5 (the black curve), which is also compared to the analytical result in Ref. [17] (the red curve). A good match is observed, indicating that the numerical model developed in this study can capture the basic features of dynamic responses of the structures.

To evaluate the control effectiveness of the proposed mega modularized substructure, a suite of 20 recorded ground motions is selected as the external excitations in the time history response analyses, and they are listed in Table 5. Additionally, these seismic ground motions are scaled to match the pseudo-acceleration response spectrum defined in the seismic code [36]. Fig. 6 shows the pseudo-acceleration response spectra of the scaled ground motions, and their mean response spectrum agrees well with the targeted one.

Table 2Properties of the mega substructure system.

Туре	Property	Value
Primary	Inter-story stiffness K (MN/m)	363.5
structure	Mass of each story M (t)	10,000
	Total height H (m)	200
	Fundamental frequency f (Hz)	0.33
	Modal mass of the fundamental mode M (t)	10,000
	Modal stiffness of the fundamental mode K (MN/ m)	43.9
	Modal damping coefficient of the fundamental mode C (kN·s/m)	838
Secondary	Mass of the substructure of each story (t)	10,000
structure	Optimal stiffness of the substructure (MN/m)	5.5
	Optimal damping coefficient of the substructure (MN-s/m)	6.4

Table 3Properties of the modular substructure in the mega modularized substructure.

Property	Value
Mass of each super module m (t)	10000/6
Optimal stiffness of modular substructure k (MN/m)	2.1
Optimal damping coefficient of the modular substructure c (MN. s/m)	2.5

Table 4Geometrical information and material properties of the primary structure.

Property	Value
Height of each floor (m)	50
Section size of the mega column (m)	5.07×5.07
Section size of the mega beam (m)	$8.46 \times 8.46*$
Material density of the primary structure (t/m3)	2.5
Young's modulus of the material (MPa)	3.45×10^{4}
Span length (m)	20

^{*} Please note these values are not for a single column or beam in real practice, they are equivalent values in the numerical model to make the dynamic characteristics of the structure identical to those in [17].

5. Numerical results

5.1. Dynamic responses

5.1.1. Primary structural responses

To systematically examine the control effectiveness of the proposed method, the seismic responses of the mega modularized substructure are calculated with the numerical model developed in Section 4. For comparison, the responses of the uncontrolled structure (UNC, the prototype structure in Fig. 3(a)) and the mega substructure are also calculated. Fig. 7 shows the top inter-story drift time histories (i.e., the drift between the 3rd and 4th floors of the primary structure) and the corresponding fast Fourier transform (FFT) spectra in different structural systems subjected to a typical ground motion (No. 6 as listed in Table 5). The peak and corresponding root mean squared (RMS) values are tabulated in Table 6.

As depicted in Fig. 7 and Table 6, both the mega modularized substructure and mega substructure system show control effectiveness over the uncontrolled counterpart, featured by lower peaks and quicker vibration decay. In particular, the maximum top inter-story drift of the mega substructure is 0.051 m, and the reduction ratio is 71.82 % compared to the uncontrolled structure (0.181 m). When the mega modularized substructure is applied, the peak top inter-story drift is further reduced to 0.036 m with a reduction ratio of 80.11 %. The frequency results in Fig. 7(b) show the same trend as those observed in the time domain. It can be seen that the first mode of the primary structure is obviously mitigated when the mega systems are used. Moreover, for the uncontrolled structure, another obvious peak occurs at about 1.25 Hz,

which corresponds to the third vibration mode of the uncontrolled structure. For the mega substructure or mega modularized substructure, the vibration induced by this vibration mode is also obviously mitigated. It is worth noting that the connecting devices between the primary and secondary structures are designed based on the fundamental vibration mode as discussed in Section 3.2, however, the results show that the higher vibration mode can also be suppressed. In other words, though the connecting devices are not purposely designed to control the higher vibration mode, this system is very robust and able to control the higher vibration mode. This is caused by the large mass ratio between the secondary and primary structures (1.0 as discussed in Section 3): many previous studies (e.g., [37]) have demonstrated that a large mass ratio can enhance the robustness of the TMD system.

To provide more insight into the control effectiveness of the mega modularized substructure subjected to different seismic ground motions, Fig. 8 presents the reduction ratios of the peak and RMS values of the top inter-story drift when the building is controlled by two mega systems. As shown, the average reduction ratio of the maximum top inter-story drift under the control of the mega modularized substructure is about 77.47 % (the black dashed line in Fig. 8(a), which is 5.56 % higher than that of the mega substructure system (the red dashed line in Fig. 8(a)). Similarly, the average reduction ratios of the RMS top inter-story drift are 81.53 % for the mega modularized substructure (the black dashed line in Fig. 8(b)) and 76.25 % for the mega substructure (the red dashed line in Fig. 8(b)), respectively. These results demonstrate the superior control effectiveness of the mega modularized substructure over the mega substructure.

5.1.2. Secondary structural responses

To examine the secondary structural response, Fig. 9 presents the inter-story drift and absolute acceleration time histories of the secondary structures on the third floor of the primary structure for the two mega systems when subjected to the No. 6 ground motion, and Table 7 tabulates the corresponding peak and RMS values. It should be noted that all the inter-story drifts are relative to the responses of the third floor of the corresponding primary structure. Moreover, the three super modules in the mega modularized substructure system in the same layer move together (i.e., no relative deformation is developed between different modules in the same layer) due to the same connection properties. In other words, the two-layer super modules behave like two TMDs in series.

As shown in Fig. 9 and Table 7, the responses of the secondary structures in different mega systems follow the same trend and are close to each other. In particular, the inter-story drift of the secondary structure in the mega substructure system is generally between the responses of upper-layer and lower-layer super modules in the mega modularized substructure system. Moreover, for the inter-story drifts, the upper-layer response is larger than that of the lower-layer super modules, while the opposite trend is observed for the absolute acceleration response. This is actually expected, and they are determined by the relative locations of the secondary structures as shown in Fig. 4. For the other earthquake ground motions, the same trends are observed, thereby, they are not shown herein for conciseness.

5.2. Robustness of the mega modularized substructure

To investigate the control robustness of the proposed mega modularized substructure, this section assumes the malfunction of certain super modules. For the sake of simplicity, three cases are considered. In Case 1, the super modules on the first floor are not functioning; in Case 2, the super modules on the second floor malfunction; and in Case 3, the super modules on the third floor are not functioning properly. For comparison, the robustness of the conventional mega substructure is also analyzed, with the substructure on the corresponding floor losing control capability. In each case, the malfunction of modules is considered by replacing the inter-module connection elements with the rigid

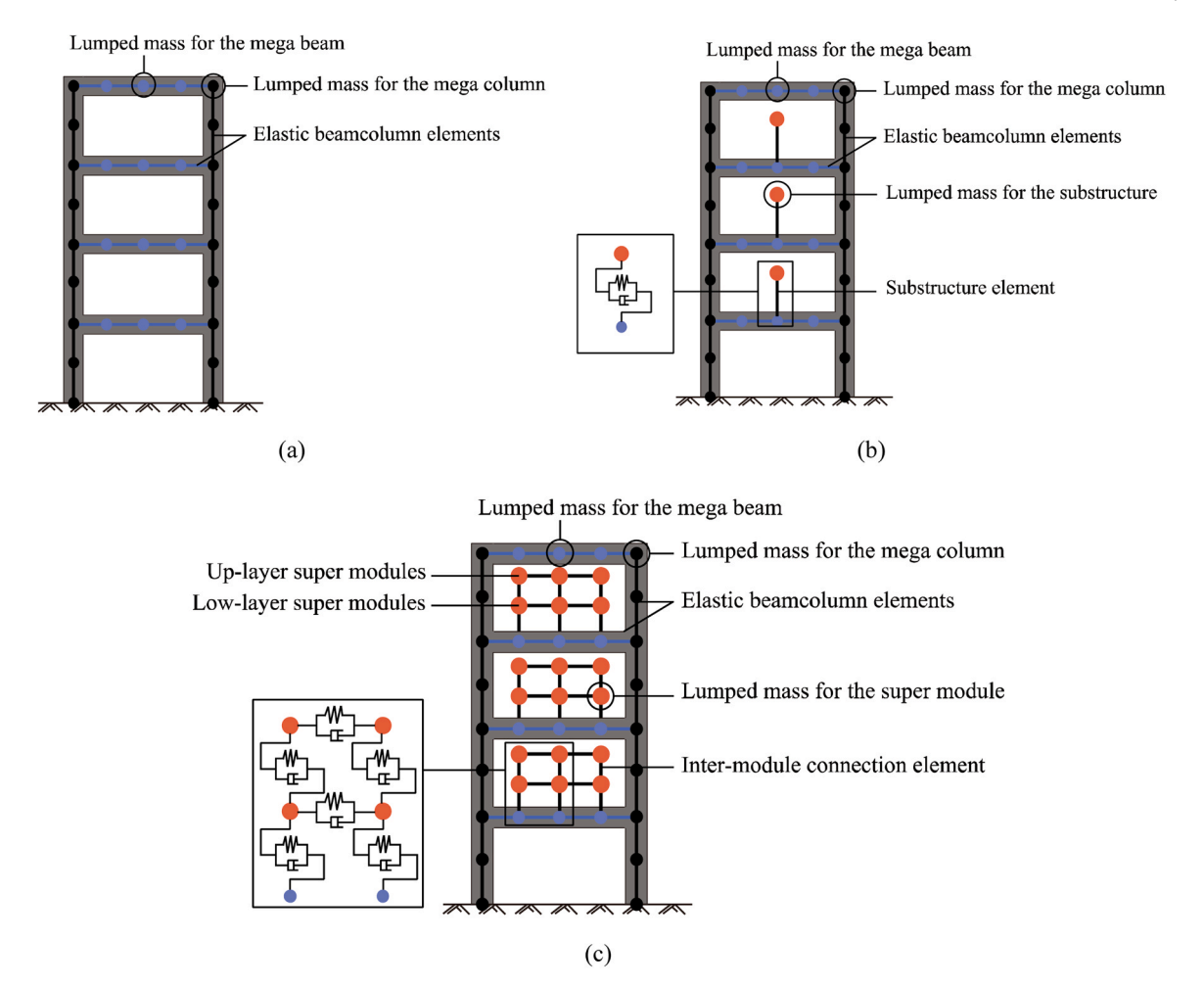


Fig. 4. Finite element models of (a) prototype structure, (b) mega substructure system, and (c) mega modularized substructure.

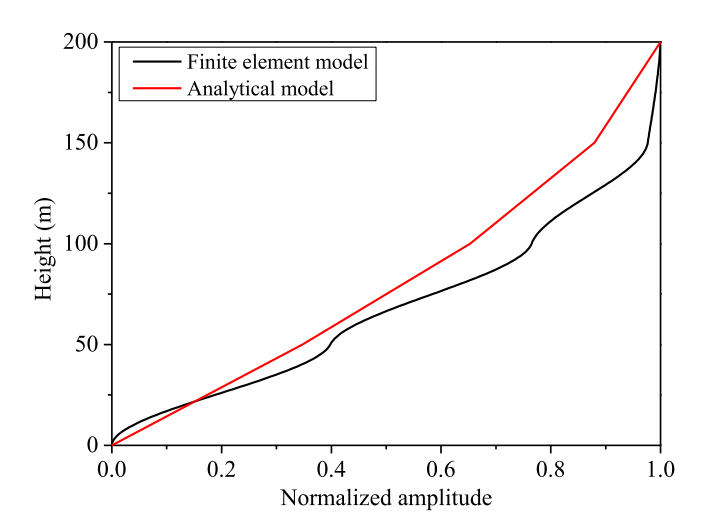


Fig. 5. Normalized fundamental mode shapes of the primary structure.

link constraint as shown in Fig. 10. In other words, the mass of the modules is lumped to the corresponding floors.

Table 8 tabulates the average RMS top inter-story drifts of the primary structure and the corresponding reduction ratios for different scenarios. For comparison, the results corresponding to the original structure (i.e., no malfunction) are also given in the table. As shown in the table, the control effectiveness is reduced as expected, when either some super modules or the substructures do not function properly as

TMDs as compared to the case with all the super modules and substructures functioning as TMDs. However, due to the contribution of the functioning super modules or substructures on the other floors, these cases still exhibit control effectiveness on the primary structure interstory drift. The results demonstrate the robustness of the two mega systems. In particular, among these three cases, Case 3 is the least effective. This is because the optimized parameters of the two mega systems are tuned to the fundamental mode of the primary structure as discussed in Section 3, and the modal amplitude increases with height as shown in Fig. 5. Therefore, among the three cases, the super modules and substructure are installed at the location with the maximum modal amplitude in Case 3, and the malfunctioning of the super modules or substructure as TMDs will evidently influence the control effectiveness. Conversely, the control effectiveness is least influenced in Case 1 since the super modules and substructure are installed at the location with minimum modal amplitude.

Notably, among these three cases, the control effectiveness of the mega modularized substructure is better than that of the mega substructure. For example, in Case 3, the average RMS top inter-story drifts of the primary structure are 0.015 m and 0.016 m for the mega modularized substructure and mega substructure with the reduction ratios being 71.15 % and 69.23 %, respectively. These results indicate that the mega modularized substructure has better control robustness over the conventional mega substructure.

Table 5Details of the selected ground motions.

No.	Earthquake event	Year	Magnitude	Epicentral distance (km)	Station	PGA (g)	Scaling factor
1	Loma Prieta	1989	6.9	28.2	Agnews State Hospital	0.159	2.67
2				14.5	Capitola	0.443	0.53
3				14.4	Gilroy Array #3	0.367	0.69
4				16.1	Gilroy Array #4	0.212	1.29
5				24.2	Gilroy Array #7	0.323	0.95
6				28.2	Hollister City Hall	0.215	0.87
7				25.8	Hollister Differential Array	0.279	1.09
8				28.8	Sunnyvale- Colton Ave.	0.209	1.23
9	Northridge	1994	6.7	15.8	Canoga Park -Topanga Can.	0.42	0.45
10	C			23.9	LA- N Faring Rd.	0.242	0.66
11				29.5	LA- Fletcher Dr.	0.24	0.69
12				25.4	Glendale- Las Palmas	0.206	1.78
13				25.5	LA – Holywood Stor FF	0.358	0.76
14				22.3	La Crescenta- New York	0.159	1.65
15				13	Canyon Country - W Lost Cany	0.482	0.31
16				12.3	Sun Valley – Roscoe Blvd	0.443	0.95
17	San Fernando	1971	6.6	21.2	LA- Hollywood Stor Lot	0.174	2.89
18	Superstition Hills	1987	6.7	13.9	EI Centro Imp. Co. Cent	0.258	0.80
19	-			24.4	Wildlife Liquef. Array	0.207	1.17
20				13.3	Westmorland Fire Station	0.211	1.03

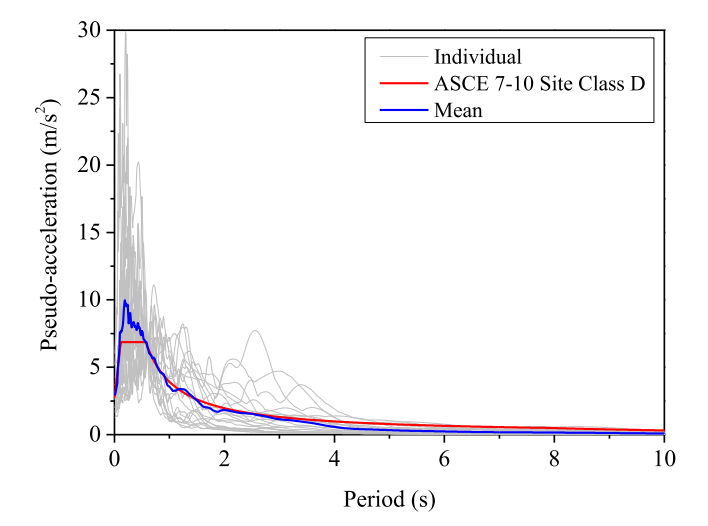


Fig. 6. Pseudo-acceleration response spectra of the selected ground motions.

5.3. Responses of the primary and secondary structures considering pounding

Pounding between adjacent structures induced by seismic excitations has been well-documented in earthquake events such as the 1994 Northridge earthquake [38], with the potential to cause severe damage to adjacent structures. Consequently, extensive studies have been conducted to investigate pounding on structural responses and to develop measures to preclude pounding [39–41]. However, studies on pounding for modular structures are rarely reported. Under strong ground motions, the mega modularized substructure proposed in this study may experience pounding between modules and/or between modules and the primary structure, potentially amplifying the response of the

Table 6Peak and RMS top inter-story drifts of the primary structure under the No. 6 ground motion.

Туре	Peak top inter-story drift (m)	RMS top inter-story drift (m)	
UNC	0.181	0.078	
Mega substructures	0.051	0.014	
Mega modularized substructure	0.036	0.012	

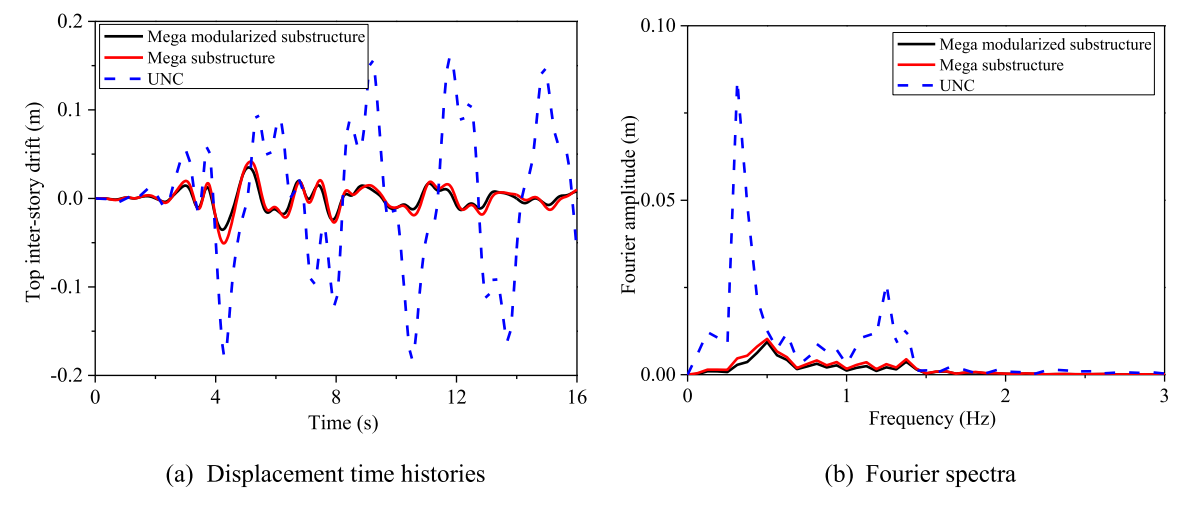


Fig. 7. Top inter-story drift time histories of the primary structure in different structural systems under a typical ground motion and the corresponding FFT spectra.

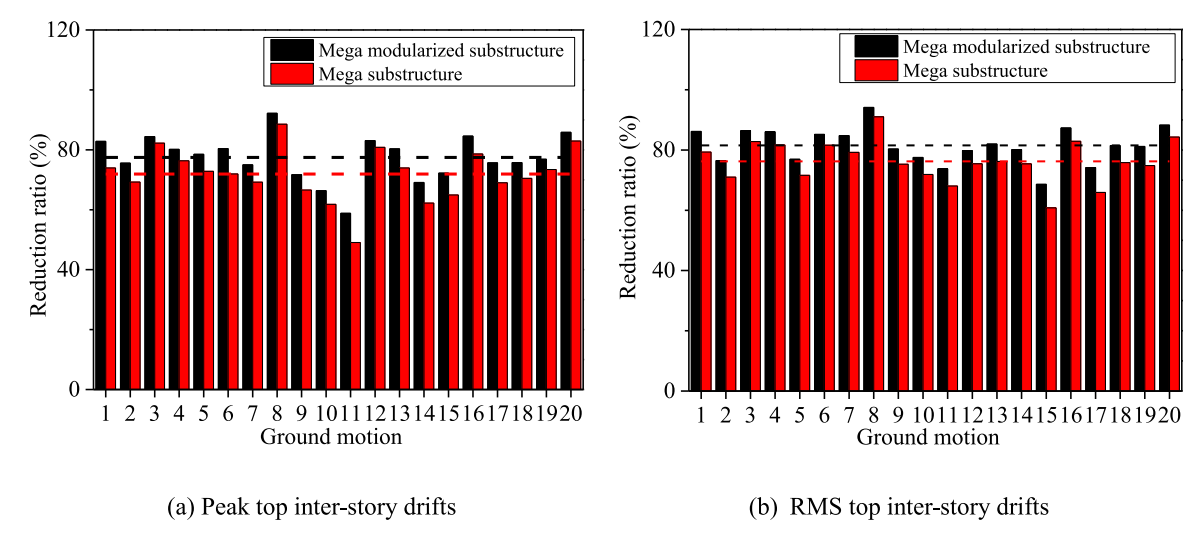


Fig. 8. Reduction ratios of the peak and RMS top inter-story drifts under different earthquake ground motions.

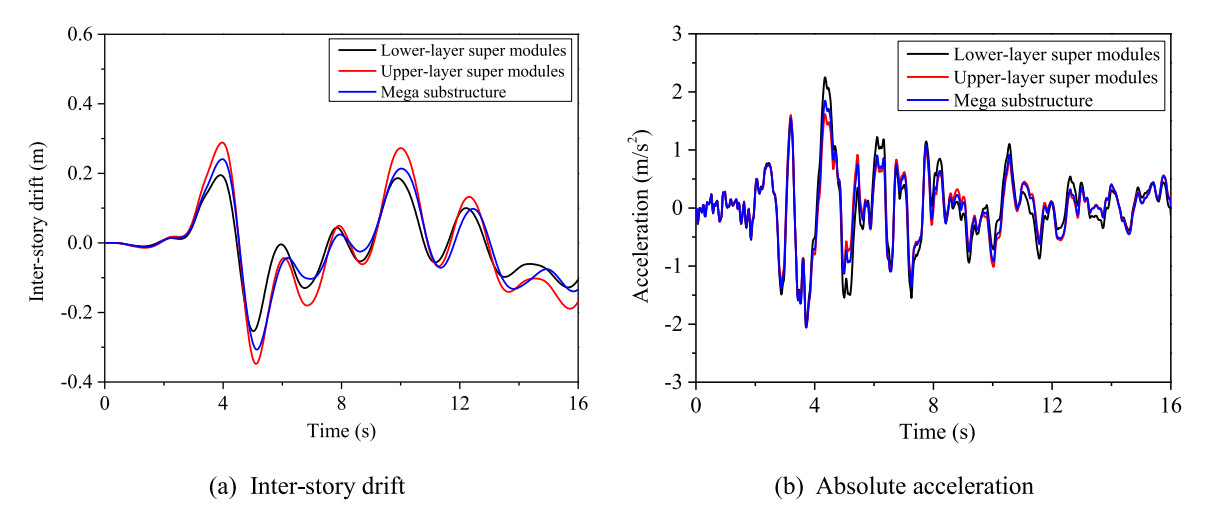


Fig. 9. Inter-story drift and absolute acceleration time histories of the secondary structure(s) on the third floor subjected to the No. 6 ground motion.

 Table 7

 Peak and RMS inter-story drifts and absolute accelerations of the secondary structure(s) on the third floor subject to the No. 6 ground motion.

Туре		Peak inter-story drift (m)	Peak absolute acceleration (m/s²)	RMS inter-story drift (m)	RMS absolute acceleration (m/s ²)
Mega substructure Mega modularized substructure	Lower-layer super modules	0.307 0.254	2.060 2.250	0.111 0.095	0.591 0.660
	Upper-layer super modules	0.348	2.057	0.138	0.570

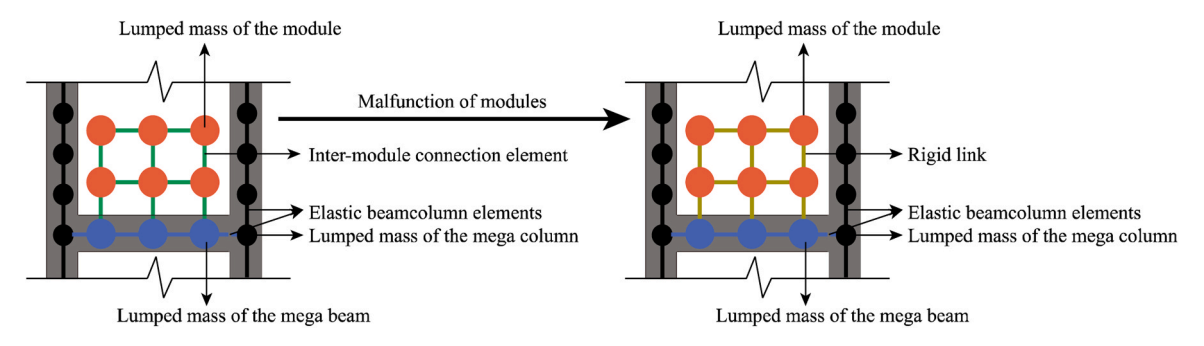


Fig. 10. Illustration of the malfunction of modules.

Table 8Average RMS value of the top inter-story drifts of the primary structure and the corresponding reduction ratios.

Type	RMS (m)		Reduction ratio (%)	
	Mega modularized substructure	Mega substructure	Mega modularized substructure	Mega substructure
Original	0.008 (\pm 0.005 *)	0.010 (± 0.007)	84.62**	80.77
Case 1	0.008 (\pm 0.006)	0.012 (± 0.008)	84.62	76.92
Case 2	0.010 (\pm $0.007)$	0.013 (± 0.011)	80.77	75.00
Case 3	0.015 (\pm 0.015)	0.016 (± 0.015)	71.15	69.23

^{*} The value in parentheses denotes the standard deviation.

primary structure and compromising the control effectiveness. As mentioned above, the control effect of the mega modularized substructure depends on the energy dissipated by the modular substructure. When pounding is considered, the secondary structural responses will be influenced, further causing an effect on the primary structural responses. Given these concerns, this section investigates the effect of pounding on the seismic responses of mega modularized substructure.

5.3.1. Numerical model incorporating pounding

In general, there are two methods to simulate pounding: the restitution coefficient and the contact element methods [42]. Among these methods, the contact element method is widely adopted since it can capture the pounding force and can be conveniently applied in the commonly used commercial software. Various contact elements have been proposed by researchers such as the linear spring model and the Kelvin model [38–40]. In the present study, the linear spring model [43]

is utilized to simulate pounding. The pounding model consists of a spring with a large impact stiffness and an initial gap. The spring is activated when the relative displacement exceeds the initial gap and the pounding force is increased linearly with respect to the relative displacement. It should be noted that energy dissipation during the pounding process is ignored in this model. Many previous studies (e.g., [44]), however, demonstrated that this simplification will not obviously influence the structural responses considering pounding generally lasts for a very short time. However, the dissipated energy during pounding could be considered using more sophisticated models like the linear viscoelastic model [45].

Fig. 11 shows the finite element model of the mega modularized substructure incorporating pounding. As shown, both the poundings between modules and the primary structure and between the intermodules are considered. For the pounding between the super modules, when the relative displacement $(u_1 - u_2)$ is smaller than the initial space (g_{p1}) , the connecting springs and dashpots (k and c) govern the structural responses as investigated in the above sections. Once the relative displacement exceeds the initial space, the adjacent super modules will come in contact and the stiffness will increase substantially to $k_{I1} + k$. For the pounding between the super modules and the primary structure, the linear contact element with a stiffness of k_{I2} will be activated when the relative displacement between the super modules and the primary structure $(u_3 - u_4)$ exceeds the initial gap (g_{p2}) , and there is no interaction/pounding when the relative displacement is smaller than the initial gap.

To simulate pounding, it is crucial to determine the appropriate impact stiffness (k_{I1} and k_{I2}). Previous studies (e.g., [41,46]) revealed that structural response is relatively insensitive to the changes in the impact stiffness. Therefore, a large value of 1.0×10^6 kN/m is adopted for the pounding stiffness in this study, i.e., $k_{I1} = k_{I2} = 1.0 \times 10^6$ kN/m. As for the initial space (g_{p1}) and initial gap (g_{p2}), they are both assumed to be 0.02 m in this study.

5.3.2. Pounding effect on the primary structural responses

Fig. 12 shows the top inter-story drifts and the corresponding Fourier

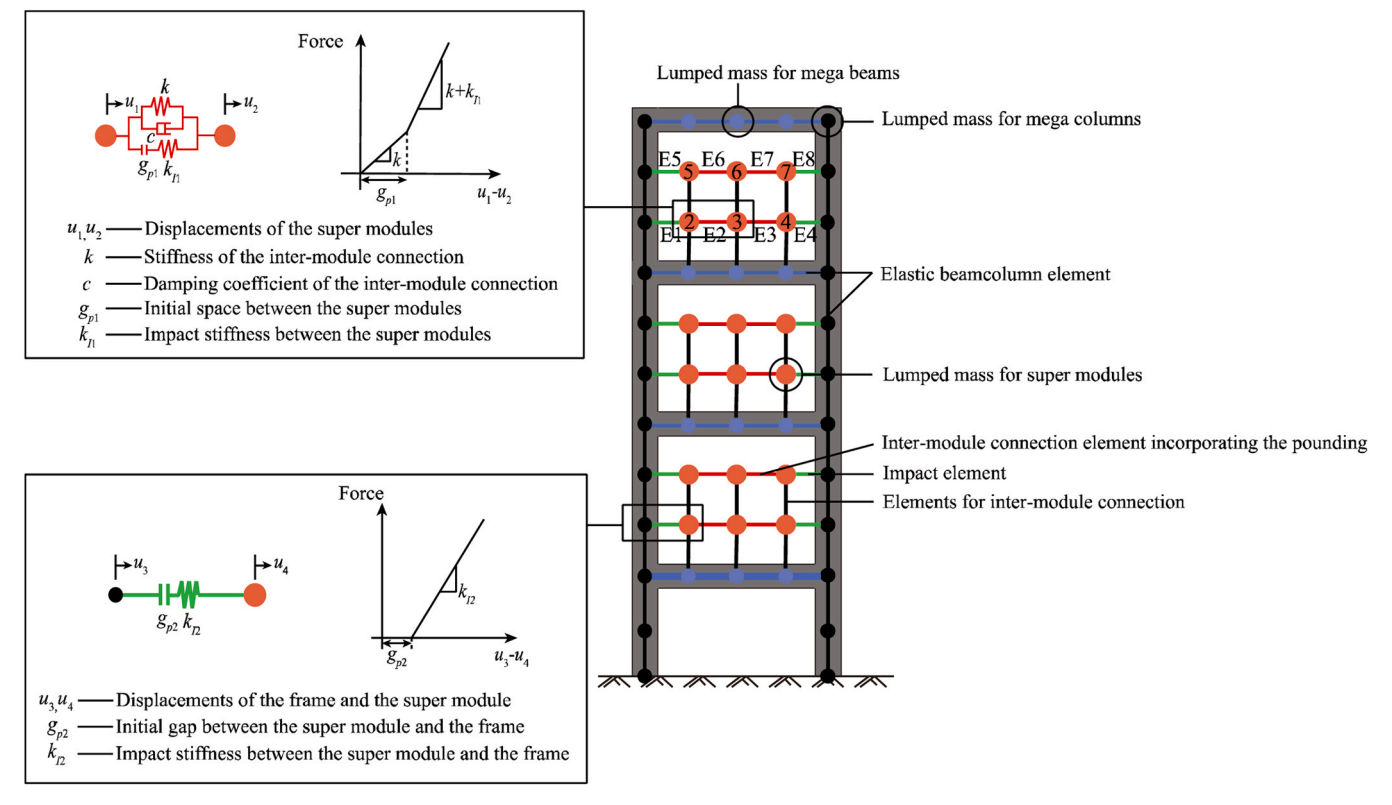


Fig. 11. Numerical model of the mega modularized substructure incorporating pounding.

^{**} The reduction ratio is calculated with respect to the response of the uncontrolled counterpart.

amplitudes of the primary structure in the mega modularized substructure under the No.6 ground motion when pounding is considered. For comparison, the results of the uncontrolled and no-pounding case are also presented. As shown in Fig. 12 (a), pounding amplifies the top inter-story drifts of the primary structure, thereby, reducing the control effectiveness. Specifically, without pounding, the peak top inter-story drift of the primary structure is 0.036 m with a reduction ratio of 80.11 % compared to the uncontrolled case. When pounding is considered, the peak top inter-story drift is increased to 0.061 m, and the reduction ratio is decreased to 66.30 %. Fourier amplitudes of the top inter-story drifts are shown in Fig. 12 (b). It can be seen that the results are consistent with those in the time domain (i.e., Fig. 12 (a)). The main reason is that, as will be shown in Section 5.3.3, pounding constrains the movements of the modules, namely the deformation of the tuned mass in the TMD system. On the other hand, it is well-known that the working mechanism of TMD is to allow large vibration of the tuned mass to dissipate seismic energy. Since TMD vibration is constrained, the control effectiveness is thus reduced.

To obtain more general conclusion on pounding effect, Fig. 13 illustrates the reduction ratios of the peak and RMS top inter-story drifts of the primary structure under all the selected ground motions. As shown, in the absence of pounding, the average reduction ratio of the peak top inter-story drift is approximately 77.47 % (the black dashed line in Fig. 13 (a)). When pounding is considered, the average reduction ratio is decreased to 64.18 % (the red dashed line in Fig. 13 (a)). Similarly, the average reduction ratios of the RMS top inter-story drift are 81.53 % for the model without pounding (the black dashed line in Fig. 13 (b)) and 70.41 % for the model with pounding (the red dashed line in Fig. 13 (b)), respectively.

The above results indicate that the control effectiveness is generally reduced when pounding is considered. However, Fig. 13 (a) also shows that, under the No.9 and No.18 ground motions, the reduction ratios of the peak top inter-story drifts of the primary structure with pounding are increased compared to those without pounding. This result can also be explained by the energy dissipated by the connecting device (the dashpots), which can be calculated as follows [47]:

$$E_{\rm s} = \sum_{i=1}^{N_{total}} \int_0^{t_{total}} c v_i^2 dt \# \tag{14}$$

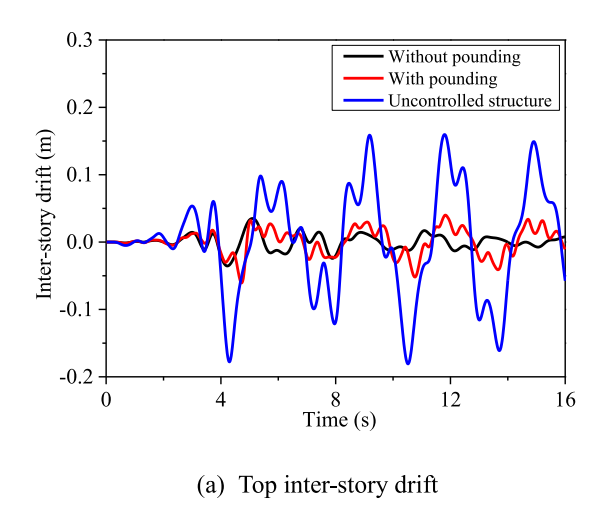
where N_{total} is the total number of the dashpots, t_{total} is the duration of the ground motion, v_i is the relative velocity of the ith device. Since the structural response is generally dominated by the first vibration mode as shown in Fig. 12 (b), and the first vibration mode amplitude increases with height as shown in Fig. 4, only the cumulative energy dissipated by the secondary structure on the third floor is calculated and N_{total} is thus

10 as shown in Fig. 11. Fig. 14 presents the cumulative energy dissipated by the secondary structure on the third floor when the structure is subjected to one of the two "abnormal" ground motions (No. 9). For comparison, one of the "normal" cases (No. 6) is also compared. As shown, under the No. 6 ground motion, the cumulative energy dissipated by the secondary structure with pounding is smaller than that without pounding, control effectiveness is thus less pronounced. However, when the structure is excited by the No.9 ground motion, the cumulative energy dissipated by the secondary structure is higher than the case without pounding in the initial stage (approximately 0–10 s), which leads to the more evident control effectiveness since the peak responses occur within this duration.

In summary, under most of the earthquake excitations, pounding generally reduces the control effectiveness. However, it may be beneficial under some other earthquake ground motions. The control effectiveness is governed by the energy dissipated by the modular substructure.

5.3.3. Pounding effect on the secondary structural responses

Fig. 15 shows the inter-story drift and absolute acceleration time histories of the secondary structure on the third floor in the mega modularized substructure with and without pounding under the No.6 ground motion. The corresponding peak and RMS values are tabulated in Table 9. As shown in Fig. 15 (a)-(b), pounding reduces the inter-story drifts of the secondary structure, which verifies the discussion in the above section that the movements of super modules are constrained. Notably, in contrast to the model without pounding where the super modules at the same layer move together, the presence of pounding results in the out-of-phase vibration among the super modules, i.e., relative displacements occur between the super modules at the same layer (see the 2nd-7th modules in Fig. 15 (a)-(b)). However, as shown in Fig. 15 (c)-(d), the absolute acceleration is significantly amplified when pounding occurs. For example, without pounding, the maximum interstory drift and absolute acceleration of the upper-layer super modules are 0.348 m and 2.057 m/s², respectively. When pounding is considered, the maximum inter-story drift is reduced to 0.126 m, while the absolute acceleration is increased to 13.565 m/s². Similar results are observed for the lower-layer super modules. With further observation of Fig. 15, it can be found that when the structural responses are small in the initial stage, the responses of the secondary structures with or without considering pounding are the same, implying no pounding occurs in the initial stage (about 0-3 s) as shown in Fig. 15 (e)-(f). However, when pounding occurs, the secondary structural inter-story drifts are reduced due to the constraint. Conversely, large absolute acceleration is induced at the pounding instants owing to the large pounding force. Since the pounding force lasts for a short time, large accelerations



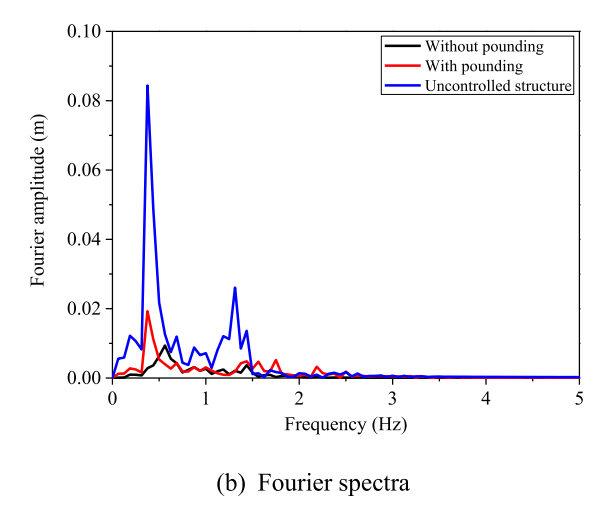


Fig. 12. Pounding effect on the top inter-story drifts of the primary structure with the corresponding Fourier amplitudes under the No.6 ground motion.

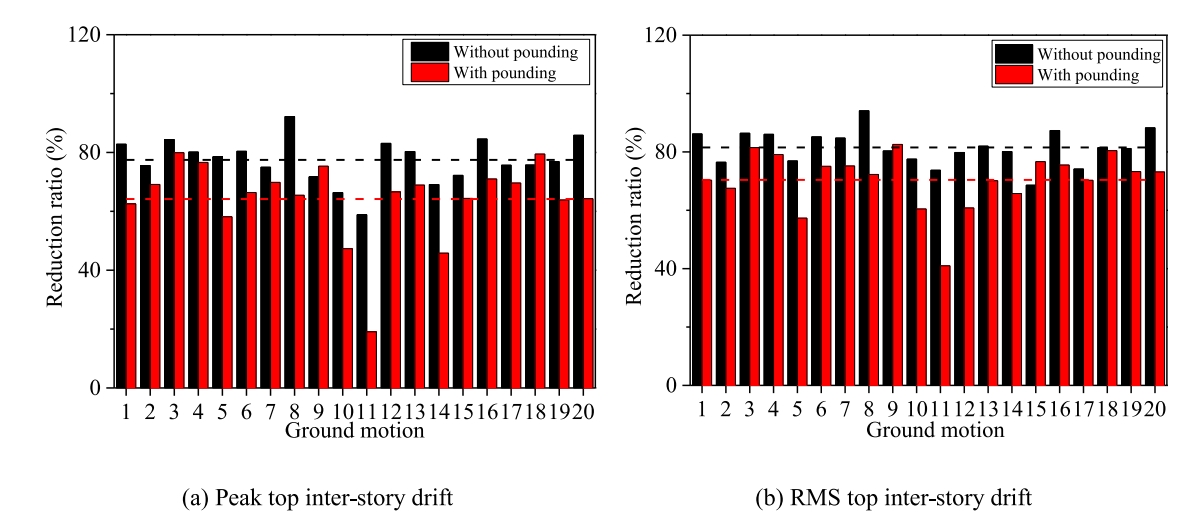


Fig. 13. Comparison of the reduction ratios on the peak and RMS top inter-story drifts of the primary structure with and without the pounding.

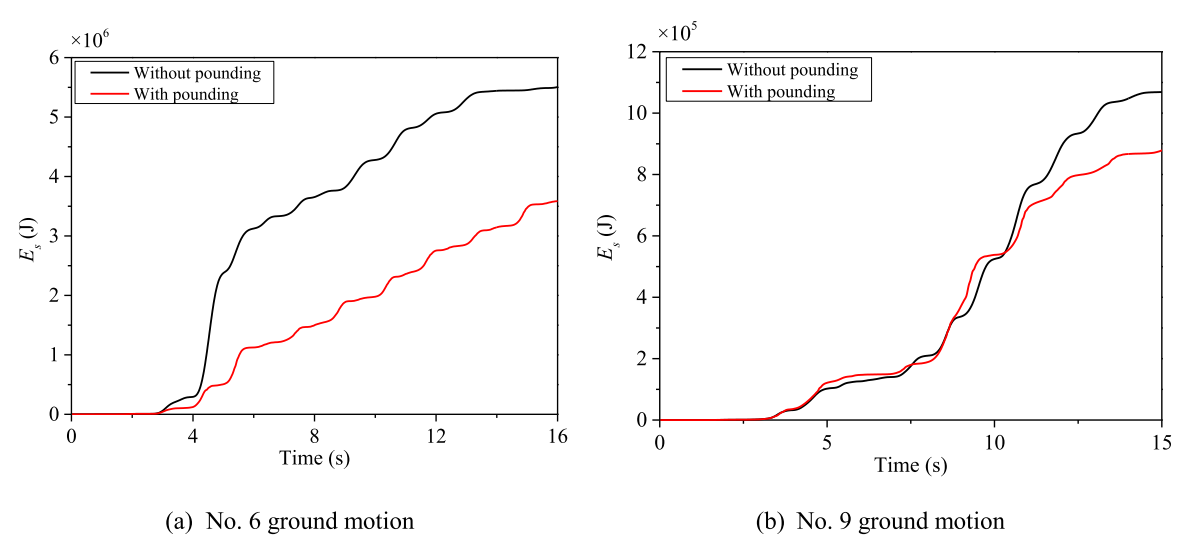


Fig. 14. Cumulative energy dissipated by the secondary structure on the third floor.

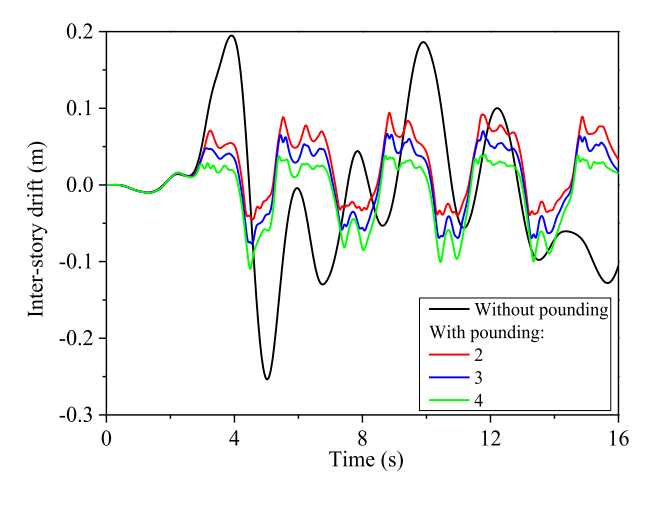
have very short duration, which have slight effect on overall structural responses as shown in Fig. 12 although they may cause localized damage to structures at the pounding locations.

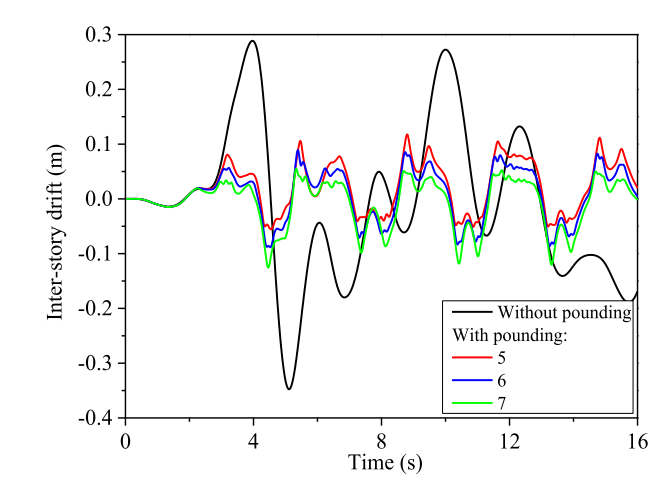
6. Conclusions

Modular construction techniques offer significant advantages such as enhanced quality control, accelerated construction speed, and reduced environmental impact compared to conventional onsite methods. These benefits can be maximized in high-rise buildings due to the use of repeatable prefabricated modules. However, the widespread application of modular construction in high-rise buildings is hindered by the lack of reliable structural systems. To address this challenge, the present study proposes a novel structural system tailored for modular high-rise buildings: the mega modularized substructure. In contrast to the flexible substructure of conventional mega substructures, the innovative mega modularized substructure features a flexible modular design of the substructure. The equations of motion of the system are developed, optimal parameters for the connection device are obtained, and systematical investigations are performed to examine the effectiveness of the proposed design. Moreover, the control robustness and pounding effect on the dynamic responses are also investigated. The following conclusions are obtained based on the analytical studies:

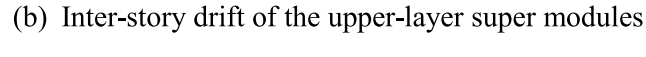
- (1) Compared to the conventional mega substructure, the proposed mega modularized substructure shows the potential to mitigate the primary structural response at the expense of increased secondary structural responses under seismic loads.
- (2) The proposed control system demonstrates better robustness against malfunction of the substructure over the conventional mega substructure, which is crucial for maintaining control effectiveness during seismic ground motions.
- (3) Pounding has significant effect on the primary structural response, which is dependent on the dissipated energy of the secondary structure. When the dissipated energy is increased, the primary structural response is mitigated.
- (4) When pounding is considered, the inter-story drift of the secondary structure is reduced. However, the sudden collision causes increased acceleration to the substructure owing to the impulsive pounding force, which may cause some localized damage to structures at the pounding locations, but its effect on overall structural response is not prominent due to the very short impulsive loading duration.

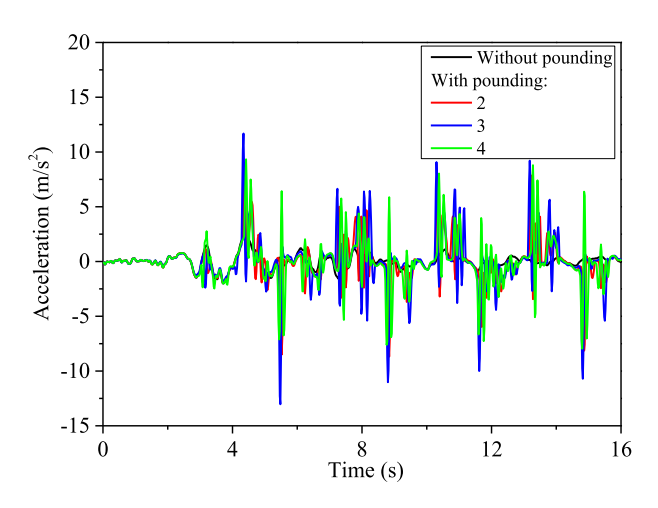
Overall, the novel mega modularized substructure proposed in the present study exhibits enhanced control effectiveness compared to the conventional mega substructure, ensuring the structural integrity of the

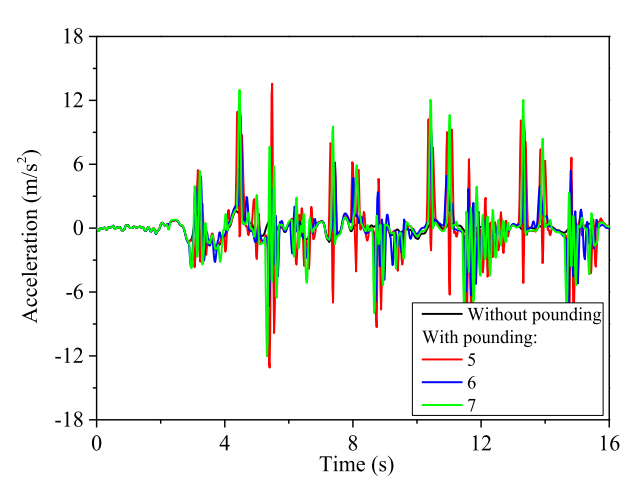




(a) Inter-story drift of the lower-layer super modules

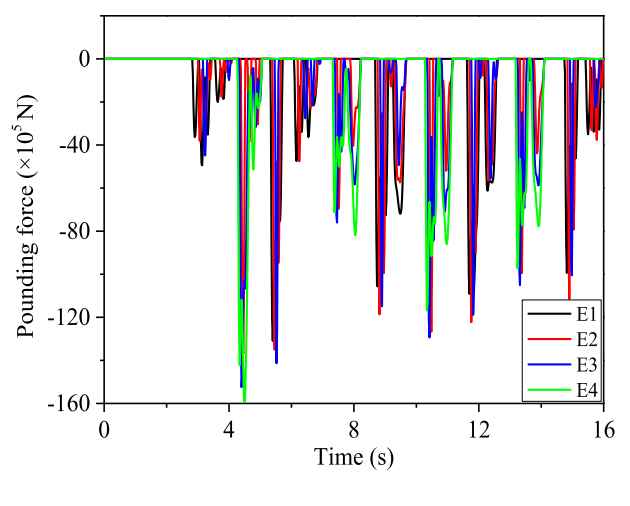


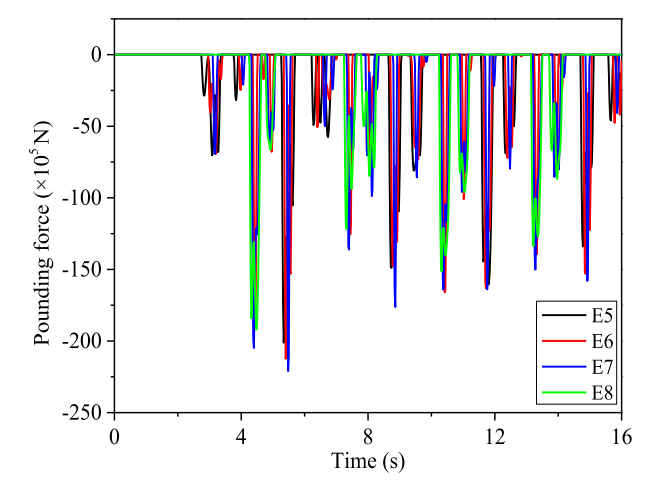




(c) Absolute acceleration of the lower-layer super modules

(d) Absolute acceleration of the upper-layer super modules





(e) Lower-layer pounding force

(f) Upper-layer pounding force

Fig. 15. Pounding effect on the secondary structural responses on the third floor under the No.6 ground motion. E1-E8 refer to the impact elements in Fig. 11.

Table 9
Peak and RMS inter-story drift and absolute accelerations of the secondary structure on the third floor under the No. 6 ground motion.

Туре		Peak inter-story drift (m)	Peak absolute acceleration (m/s²)	RMS inter-story drift (m)	RMS absolute acceleration (m/s²)
Without pounding	Lower-layer super modules	$0.254~(~\pm~0.095^*)$	$2.250~(~\pm~0.659)$	0.095	0.660
	Upper-layer super modules	$0.348~(~\pm~0.138)$	$2.057~(~\pm~0.570)$	0.138	0.570
With pounding	Lower-layer super modules	$0.110 \; (\; \pm \; 0.042)$	13.031 (\pm 2.035)	0.047	2.275
	Upper-layer super modules	$0.126~(~\pm~0.047)$	13.565 (\pm 2.402)	0.050	2.685

^{*} The value in parentheses denotes the standard deviation.

entire building under external dynamic excitations. Therefore, it provides a viable solution for modular high-rise buildings and offers a feasible approach to construct modular high-rise buildings.

CRediT authorship contribution statement

Linwei Jiang: Writing – original draft, Software, Data curation, Conceptualization. **Haoran Zuo:** Writing – review & editing. **Kaiming Bi:** Writing – review & editing, Supervision, Project administration, Funding acquisition, Conceptualization. **Hong Hao:** Writing – review & editing, Supervision. **Wensu Chen:** Writing – review & editing, Supervision.

Declaration of Competing Interest

The authors declare that they have no known competing financial interests or personal relationships that could have appeared to influence the work reported in this paper.

References

- [1] Zhu Z, Lei W, Wang Q, Tiwari N, Hazra B. Study on wind-induced vibration control of linked high-rise buildings by using TMDI. J Wind Eng Ind Aerodyn 2020;205: 104306.
- [2] Song J, Tse K. Dynamic characteristics of wind-excited linked twin buildings based on a 3-dimensional analytical model. Eng Struct 2014;79:169–81.
- [3] El-Khoury O, Adeli H. Recent advances on vibration control of structures under dynamic loading. Arch Comput Methods Eng 2013;20:353–60.
- [4] Den Hartog JP. Mechanical Vibrations. Chelmsford, MA, USA: Courier Corporation;
- [5] Konar T, Ghosh A. A review on various configurations of the passive tuned liquid damper. J Vib Control 2023;29:1945–80.
- [6] Shukla A, Datta T. Optimal use of viscoelastic dampers in building frames for seismic force. J Struct Eng 1999;125:401–9.
- [7] Jangid R. Optimum frictional elements in sliding isolation systems. Comput Struct 2000;76:651–61.
- [8] Samali B, Yang J, Yeh C. Control of lateral-torsional motion of wind-excited buildings. J Eng Mech 1985;111:777–96.
- [9] Chung L, Lin R, Soong T, Reinhorn A. Experimental study of active control for MDOF seismic structures. J Eng Mech 1989;115:1609–27.
- [10] Y. Yamadan, N. Ikawa, H. Yokoyama, E. Tachibana. Active control of structures using the joining member with negative stiffness. In Proceedings of the First World Conference on Structural Control, Los Angeles, CA, USA, 3–5 August 1994.
- [11] Hrovat D, Barak P, Rabins M. Semi-active versus passive or active tuned mass dampers for structural control. J Eng Mech 1983;109:691–705.
- [12] Patten W, Sack R, He Q. Controlled semiactive hydraulic vibration absorber for bridges. J Struct Eng 1996;122:187–92.
- [13] Dyke SJ. Modeling and control of magnetorheological dampers for seismic response reduction. Smart Mater Struct 1996;5:565.
- [14] Dimentberg M, Iourtchenko D. Random vibrations with impacts: A review. Nonlinear Dyn 2004;36:229–54.
- [15] Symans M, Constantinou M. Semi-active control systems for seismic protection of structures: A state-of-the-art review. Eng Struct 1999;21:469–87.
- [16] Bhaiya V, Bharti S, Shrimali M, Datta T. Genetic algorithm based optimum semiactive control of building frames using limited number of magneto-rheological dampers and sensors. J Dyn Syst, Meas, Control 2018;140:101013.
- [17] Feng M, Mita A. Vibration control of tall buildings using mega subconfiguration. J Eng Mech 1995;121:1082–8.
- [18] Zhang Y, Liang Q. Asynchronous driving principle and its application to vibration control. Earthq Eng Struct Dyn 2000;29:259–70.
- [19] Nakamura Y, Saruta M, Wada A, Takeuchi T, Hikone S, Takahashi T. Development of the core-suspended isolation system. Earthq Eng Struct Dyn 2011;40:429–47.

- [20] Yu Y, Chen Z. Rigidity of corrugated plate sidewalls and its effect on the modular structural design. Eng Struct 2018;175:191–200.
- [21] Jin R, Hong J, Zuo J. Environmental performance of off-site constructed facilities: A critical review. Energy Build 2020;207:109567.
- [22] Jellen A, Memari A. The state-of-the-art application of modular construction to multi-story residential building. Proc 1st Resid Build Des Constr Conf 2013: 284–93
- [23] Thai H, Ngo T, Uy B. A review on modular construction for high-rise buildings. Structures 2020;28:1265–90.
- [24] Park H, Ock J. Unit modular in-fll construction method for high-rise buildings. KSCE J Civ Eng 2016;20:1201–10.
- [25] Srisangeerthanan S, Hashemi M, Rajeev P, Gad E, Fernando S. Numerical study on the effects of diaphragm stiffness and strength on the seismic response of multistory modular buildings. Eng Struct 2018;163:25–37.
- [26] Lawson R, Ogden R. Hybrid light steel panel and modular systems. Thin-Walled Struct 2008;46:720–30.
- [27] Zuo H, Bi K, Hao H. Using multiple tuned mass dampers to control offshore wind turbine vibrations under multiple hazards. Eng Struct 2017;141:303–15.
- [28] Srisangeerthanan S, Hashemi M, Rajeev P, Gad E, Fernando S. Review of performance requirements for inter-module connections in multi-story modular buildings. J Build Eng 2020;28:101087.
- [29] Lacey A, Chen W, Hao H, Bi K. Review of bolted inter-module connections in modular steel buildings. J Build Eng 2019;23:207–19.
- [30] Ye Z, Feng D, Wu G. Seismic control of modularized suspended structures with optimal vertical distributions of the secondary structure parameters. Eng Struct 2019;183;160–79.
- [31] Xiang P, Nishitani A. Optimum design of tuned mass damper floor system integrated into bending-shear type building based on H∞, H2, and stability maximization criteria. Struct Control Health Monit 2015;22:919–38.
- [32] Pourzeynali S, Zarif M. Multi-objective optimization of seismically isolated highrise building structures using genetic algorithms. J Sound Vib 2008;311:1141–60.
- [33] Mckenna F, Scott MH, Fenves GL. Nonlinear Finite-Element Analysis Software Architecture Using Object Composition. J Comput Civ Eng 2010;24:95–107.
- [34] Sharma A, Eligehausen R, Reddy G. A new model to simulate joint shear behavior of poorly detailed beam-column connections in RC structures under seismic loads, Part I: Exterior joints. Eng Struct 2011;33:1034-51.
- [35] Shafaei J, Zareian M, Hosseini A, Marefat M. Effects of joint flexibility on lateral response of reinforced concrete frames. Eng Struct 2014;81:412–31.
- [36] ASCE. Minimum Design Loads for Buildings and Other Structures ASCE 7-10. United States of America; 2010.
- [37] Angelis M, Perno S, Reggio A. Dynamic response and optimal design of structures with large mass ratio TMD. Earthq Eng Struct Dyn 2012;41:41–60.
- [38] Maison B, Kasai K. Analysis for a type of structural pounding. J Struct Eng 1990; 116:957–77
- [39] Anagnostopoulos S. Equivalent viscous damping for modeling inelastic impacts in earthquake pounding problems. Earthq Eng Struct Dyn 2004;33:897–902.
- [40] Pantelides C, Ma X. Linear and nonlinear pounding of structural systems. Comput Struct 1998;66:79–92.
- [41] Muthukumar S, DesRoches R. A Hertz contact model with non-linear damping for pounding simulation. Earthq Eng Struct Dyn 2006;35:811–28.
- [42] Chen J, Han Q, Liang X, Du X. Effect of pounding on nonlinear seismic response of skewed highway bridges. Soil Dyn Earthq Eng 2017;103:151–65.
- [43] Madani B, Behnamfar F, Riahi HT. Dynamic response of structures subjected to pounding and structure-soil-structure interaction. Soil Dyn Earthq Eng 2015;78: 46–60
- [44] Shrestha B, Hao H, Bi K. Effectiveness of using rubber bumper and restrainer on mitigating pounding and unseating damage of bridge structures subjected to spatially varying ground motions. Eng Struct 2014;79:195–210.
- [45] Polycarpou P, Komodromos P. On poundings of a seismically isolated building with adjacent structures during strong earthquakes. Earthq Eng Struct Dyn 2010;39: 933–40.
- [46] Maison B, Kasai K. Analysis for type of structural pounding. J Struct Eng 1990;116: 957–77.
- [47] Jiang S, Bi K, Ma R, Xu K. H∞ closed-form solution of tuned mass damper enhanced with negative stiffness element (TMD-NS) for structural vibration control. J Sound Vib 2024;586:118510.